Hindawi Publishing Corporation
Advances in Materials Science and Engineering
Volume 2013, Article ID 686409, 8 pages
http://dx.doi.org/10.1155/2013/686409

Research Article

Performance Analysis of Al_2O_3/Water Nanofluid with Cationic Chitosan Dispersant

T. Y. Chen,[1] H. P. Cho,[2] C. S. Jwo,[1] and L. Y. Jeng[3]

[1] *Department of Energy and Air-Conditioning Refrigeration Engineering, National Taipei University of Technology, Taipei City 10608, Taiwan*
[2] *Department of Mechanical Engineering, National Taiwan University, Taipei City 10617, Taiwan*
[3] *Graduate Institute of Mechanical and Electrical Engineering, National Taipei University of Technology, Taipei City 10608, Taiwan*

Correspondence should be addressed to T. Y. Chen; t100459002@ntut.edu.tw

Received 15 September 2013; Accepted 23 October 2013

Academic Editor: Ho Chang

This study aimed to investigate the effect of the cationic chitosan dispersant on the thermal conductivity, dispersion, and the suspension of 15 nm Al_2O_3/water nanofluid. The study employed two-step method to mix the Al_2O_3 powder, deionized water, and dispersant to conduct an experiment of the settling properties and thermal conductivity of nanofluid in a stable environment, analyzing the adhesion of nanofluid to copper pipe walls in practical operations. The results indicated that 1.0 wt.% Al_2O_3/water nanofluid with 0.05 wt.% cationic chitosan dispersant increased its thermal conductivity up to 4.1% and 12.6% compared with nanofluid with deionized water at the temperature of 15°C and 55°C. At the flow ratio of 2 L/min, the overall heat conductivity improved by 8.3% and 17.4%, respectively, under 60 W and 150 W heating power. The solution performed better in dispersion and suspension than that in the original sample with no cationic chitosan dispersant. The cationic chitosan dispersant, as a result, was proved to improve the dispersion and suspension of nanofluid. It also helped to reduce the frequency of nanoparticles sticking to the pipe wall, increasing the practicability of nanofluid.

1. Introduction

The application of nanofluid, such as application in heat pipe, heat exchanger, practical utilization of solar energy, and water cooling system, is gradually expanding [1–5]. Previous studies had already suggested adding nanoparticles to the substrate solution to increase its thermal conductivity [6–18]. However, thermal conductivity of nanofluid may not be influenced other than the particle size, agglomeration, and precipitation [12, 14, 15, 19–21]. On the other hand, the millimeter-sized and micron-sized particles added to the working fluid may lead to pipe blockage and abrasion [22]. To improve the suspension and settling properties of nanofluid and to prevent blockage possibilities of pipelines resulting from nanofluid have become important issues [23].

In 2009, Zhu et al. [24] studied the effect of the suspension behavior of Al_2O_3/water nanofluid on different pH values and different concentrations of sodium dodecylbenzene sulfonate (SDBS) dispersant on thermal conductivity. The result indicated that the stability and thermal conductivity of Al_2O_3/water nanofluid had a significant correlation with different pH values and different concentrations of SDBS dispersant. The thermal conductivity increased by 10.1% when the weight concentration of Al_2O_3 nanoparticle reached 0.0015.

Wusiman et al. [25] applied the SDBS and sodium dodecyl sulfate (SDS) dispersant to the carbon nanotube solution in 2012. These two surface-active agents enabled better dispersion and long-time stability of the fluid.

In 2012, Hung et al. [1] proposed the Al_2O_3/water nanofluid and applied the nanofluid with cationic chitosan dispersant to heat pipe operation. Such an application increased the working efficiency by 22.7%–56.3% more than the substrate solution. Dispersant helped to increase the suspension and stability of fluids; however, it also reduced the heat conductivity ratio of the fluid [1, 25].

This study employed a series of experiments in precipitation, adhesion on the metal surface, and thermal conductivity

of the fluids to discuss the influence of dispersant on the nanofluid and its practicability.

2. Interrelated Theories

2.1. Agglomeration. Agglomeration refers to a phenomenon in which single particles agglomerate with each other to reduce the surface energy in each particle. The smaller the particle is, the higher the surface energy is. Agglomeration can be divided into hard agglomeration and soft agglomeration in terms of different cohesion of particles. The chemical bonds among particles in hard agglomeration make them uneasy to disperse. There are, however, no chemical bonds among particles in soft agglomeration, resulting in looser structure than those among particles in hard agglomeration. Particles in soft agglomeration, consequently, may easily disperse into single particles [26, 27].

2.2. Dispersion Technology. There are three methods in fluid dispersion technology as follows: mechanical control, medium control, and agent control. Mechanical control applies disintegrator, ultrasonic oscillator, and electromagnetic stirring to particle dispersion. Medium control applies different mediums to different particles in terms of surface properties and like polarity to reach better dispersion effects. Agent control applies different dispersants to different particles in terms of the physical and chemical conditions of the medium to improve the rejection among particles [26, 27].

2.3. Zeta Potential. Zeta potential is an important parameter of particle suspension behavior. Due to surface energy, the well-dispersed suspended particles may agglomerate with each other, leading to precipitation. The repulsive energy of suspended nanoparticles in a solution is small, generally speaking. Agglomeration may occur when the attracting energy among particles is larger than the repulsive energy. The repulsive energy, therefore, should be improved to prevent agglomeration. As a result, a relatively high zeta potential will confer stability of nanofluid [26, 28].

2.4. Settling Rate. The experiment was designed to investigate the correlating process of changes between density and time on the fluid added with the 15 nm Al_2O_3 nanoparticles and dispersant. The density changes, based on the same fluid sample, were measured initial and final in experimental. Therefore, the ratio of the pre- and postmeasurement as well as the initial density measurement was utilized to represent the settling rate of the fluid. It is shown in

$$r_s = \frac{\rho_{\text{final}} - \rho_{\text{initial}}}{\rho_{\text{initial}}}, \tag{1}$$

where ρ_{initial} is the initial measurement density and ρ_{final} is the final measurement density.

2.5. The Overall Heat Transfer Capacity Ratio. This study employed water and 15 nm Al_2O_3 nanoparticles as the substrate solution to compare the overall heat transfer capacity ratio of solution with dispersant and solution without dispersant. The experiment was designed to calculate the differences in thermal conductivities of nanofluid and water with the same control variables and heat exchanger. The overall heat transfer capacity ratio (r_{OHTC}) in the heat exchanger can be implied by the following:

$$r_{\text{OHTC}} = \frac{U_{\text{nanofluid}}}{U_{\text{water}}} = \frac{(T_{\text{wall}} - T_m)_{\text{water}}}{(T_{\text{wall}} - T_m)_{\text{nanofluid}}}, \tag{2}$$

where T_{wall} is the mean temperature of the base plate and T_m is the average temperature of liquid traversing the heat exchange, $T_m = (T_{\text{liq.in}} + T_{\text{liq.out}})/2$.

3. Experimental

3.1. Experimental Apparatus and Procedure. The study employed the 15 nm Al_2O_3/water nanofluid with cationic chitosan dispersant to analyze the properties of nanofluid, among which the powder concentrations of the solution were 0.5 wt.% and 1.0 wt.%, and the dispersant concentrations were 0.0 wt.%, 0.05 wt.%, 0.1 wt.%, 0.3 wt.%, and 0.5 wt.%. All the samples were concocted in light of the two-level allegation. The pending experimental samples were made by operating through ultrasonic cleaner (TOHAMA, DC400, Taiwan) and electromagnetic stirrer (PC-420D, CORNING, Taiwan) 3 times each and the interval of each operation was 1 hour. Basic procedures of the experiment were listed as follows. (1) Zeta potentials of the fluid samples at the same temperature were measured by Zetasizer (Nano ZS90, MALVERN, United Kingdom). All the measured samples were selected at the fixed distance under the same fluid level and then tested in the measuring containers. (2) The fluid samples were selected from 15 cm below the fluid level every 24 hours and the density changes were measured by densitometer (DA-130N, KEM, Japan) in the consecutive 20 days. The experimental samples were placed in the environmental temperature of 25°C during the testing period. (3) The heat conductivity ratio of the fluid samples at the same temperature and fluid level was measured by thermal property analyzer (KD2, DECAGON, United States). The temperature was controlled by setting a desired temperature onto the thermostatic sink (B403L, FIRSTEK, Taiwan) and the experimental samples were then placed in it to wait until the temperature became stabilized before reaching the desired temperature. The thermostatic sink was temporarily shut down to reduce the impact of vibration on the properties during the experimental period. (4) Components of the copper pipe wall that had direct contact with nanofluid were analyzed by energy dispersive spectrometer (7852, OXFORD Instruments, UK). The copper patch was placed in the inner layer of the beaker in which the fluid sample was filled and then taken out to be examined and measured after 40-hour operation by electromagnetic heating stirrer (PC-420D, CORNING, Taiwan) under the condition of 35°C and 200 rev/min. The study aimed to investigate the disparity, suspension, thermal conductivity capacity, and applications of the nanofluid by means of the basic experimental procedures.

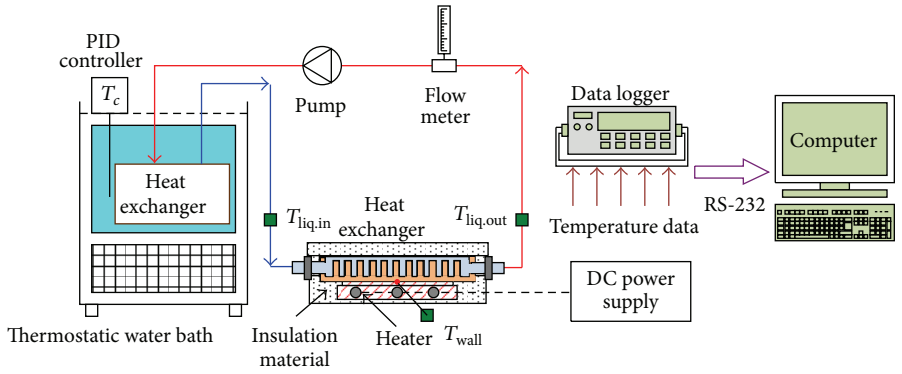

Figure 1: Layout of device in heat exchange experiment.

Table 1: Parameters in heat exchange experiment.

Items	Parameters
Volume of the fluid sample	750 mL
Inlet water temperature of heat exchanger	20°C, 40°C
Sample of fluid	Solution without dispersant: 0.5 wt.% and 1.0 wt.% Al_2O_3/water Solution with 0.05 wt.% cationic chitosan dispersant: 0.5 wt.% and 1.0 wt. % Al_2O_3/water
Heating power	60 W, 90 W, 120 W, and 150 W
Flow ratio	1 L/min and 2 L/min
Temperature	25 ± 2°C

Experiment on the overall heat transfer capacity ratio was employed by water circulating system, as shown in Figure 1, to analyze the thermal exchange capacity of the nanofluid with dispersant. Thermostatic sink was in place to supply stable inlet water temperature of heat exchanger, DC water pump (MCP-655, SWIFTECH, USA) was equipped with the flow meter to enable a constant flow ratio, and heater combined with power supply (GPC-3030DQ, GW INSTEK, Taiwan) was applied to provide stable heating power. The data was obtained and analyzed through data logger. Parameters of the experiment are shown in Table 1.

3.2. Uncertainty Analysis. The uncertainty of the experimental result was determined by the bias of experimental measurement parameters. The density was measured by the densitometer and the steel ruler was used to measure the distance from that below fluid level in the precipitation experiment. The thermal property analyzer was applied to measure thermal conductivity coefficient and T-type thermocouple was to measure fluid temperature in the thermal conductivity coefficient experiment. In the overall thermal exchange experiment, the flow was measured by flow meter and T-type thermocouple was used to measure inlet and outlet water temperatures of the fluid heat exchanger and mean temperature of the base plate. Power supply was there to provide stable heating power. The uncertainty of settling rate, heat conductivity rate, and overall heat transfer capacity ratio was displayed as follows:

$$u_{r_s} = \left(\frac{\Delta\rho_{\text{initial}}}{\rho_{\text{initial}}} + \frac{\Delta\rho_{\text{final}}}{\rho_{\text{final}}} + \frac{\Delta L}{L} + \frac{\Delta T_{\text{ambient}}}{T_{\text{ambient}}} \right)^{1/2}, \quad (3)$$

$$u_{k_{\text{nf}}/k_{\text{bf}}} = \left(\frac{\Delta k_{\text{nf}}}{k_{\text{nf}}} + \frac{\Delta k_{\text{bf}}}{k_{\text{bf}}} + \frac{\Delta T_{\text{liq.}}}{T_{\text{liq.}}} \right)^{1/2}, \quad (4)$$

$$u_{r_{\text{OHTC}}} = \left(\left[\frac{\Delta\dot{Q}}{\dot{Q}} + \frac{\Delta T_{\text{wall}}}{T_{\text{wall}}} + \frac{\Delta T_{\text{liq.in}}}{T_{\text{liq.in}}} + \frac{\Delta T_{\text{liq.out}}}{T_{\text{liq.out}}} + \frac{\Delta W}{W} \right]_{\text{water}} + \left[\frac{\Delta\dot{Q}}{\dot{Q}} + \frac{\Delta T_{\text{wall}}}{T_{\text{wall}}} + \frac{\Delta T_{\text{liq.in}}}{T_{\text{liq.in}}} + \frac{\Delta T_{\text{liq.out}}}{T_{\text{liq.out}}} + \frac{\Delta W}{W} \right]_{\text{nanofluid}} \right)^{1/2}. \quad (5)$$

The accuracy of density, steel ruler, power supply, and flow meter was ±0.001 g/cm^3, ±1 mm, ±0.1 W, and ±0.02 L/min, respectively. The maximal value of the uncertainty of experimental conditions of settling rate, heat conductivity rate, and overall heat transfer capacity ratio was ±12.6%, ±16.3% and ±28.9%, respectively, on the basis of forgoing formulas (2)–(4). Thus, the uncertainty of the experiment can be controlled at lower than ±12.6%, ±16.3%, and ±28.9%, respectively.

4. Results and Discussion

Figure 2 shows the behavior change of zeta potential of the cationic chitosan dispersant in different concentrations. The figure indicated that cationic chitosan dispersant did increase the zeta potential of nanofluid up to 24%–30%. However, the relationship between the additive amount of dispersant and zeta potential was not proportional; redundant dispersant might depress the zeta potential. The experimental result of the zeta potential suggested that dispersant did improve the dispersion of nanoparticles in fluids, whereas, particle suspension was also influential to the application of nanofluid, in which better dispersion and suspension would increase

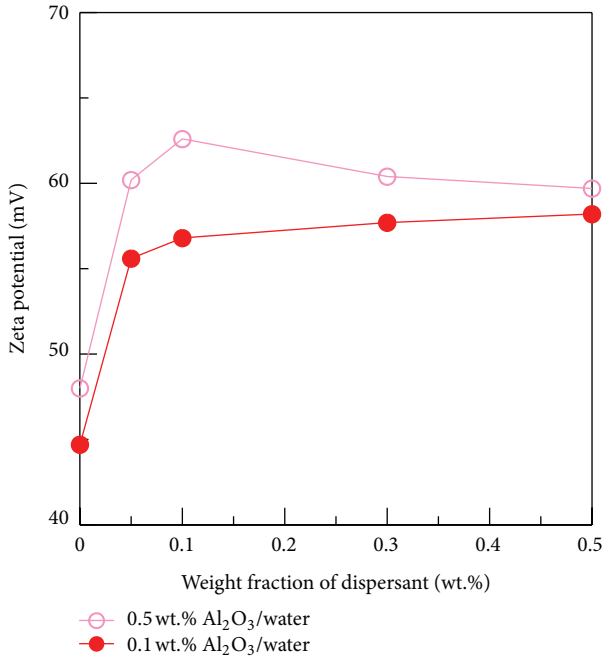

FIGURE 2: Correlation between zeta potential and weight fraction of dispersant.

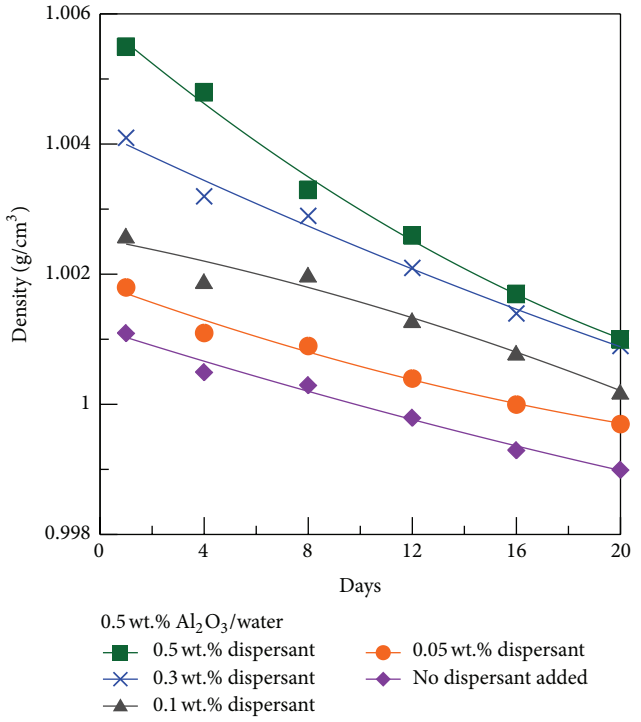

FIGURE 3: Correlation between weight concentration and precipitation behavior (0.5 wt.% Al_2O_3/water).

the stability and heat conductivity of nanofluid. Figures 3 and 4, respectively, indicate the precipitation of 0.5 wt.% and 1.0 wt.% Al_2O_3/water nanofluid in different dispersant concentrations in 20 days. The figures show that the sample with 0.5 wt.% dispersant had the most severe precipitation, while the sample with 0.05 wt.% dispersant reached better suspension; the maximum settling rates were, respectively, 0.21% and 0.26%. Considering agglomeration and precipitation, Al_2O_3/water nanofluid with 0.05 wt.% cationic chitosan dispersant was selected as the working fluid for the following procedures.

Figure 5 indicates the increment of heat conductivity ratio at different temperatures. Nanofluid with no dispersant had the most increment of heat conductivity at the same temperature and powder concentration; dispersant may drop the heat conductivity ratio and block the increment of heat conductivity by adding the nanoparticles to the fluid. 1.0 wt.% Al_2O_3/water nanofluid with no dispersant and 1.0 wt.% Al_2O_3/water nanofluid with cationic chitosan dispersant, respectively, reached 14.2% and 12.6% of conductivity increment compared with the deionized water at the temperature of 55°C. The nanofluids, respectively, reached 4.8% and 4.1% of conductivity increment at the temperature of 15°C.

Dispersion of and suspension of nanoparticles and pipe blockage may be influential to the practical application of nanofluid. Table 2 is the component analysis and surface distribution on the copper surface after 40 hours of relative operation with the nanofluid with no dispersant and with the nanofluid with 0.05 wt% cationic chitosan dispersant. Powder particles on the surface of copper pipe could be clearly seen after operating the nanofluid with no dispersant. Fluid with higher powder concentration had more significant

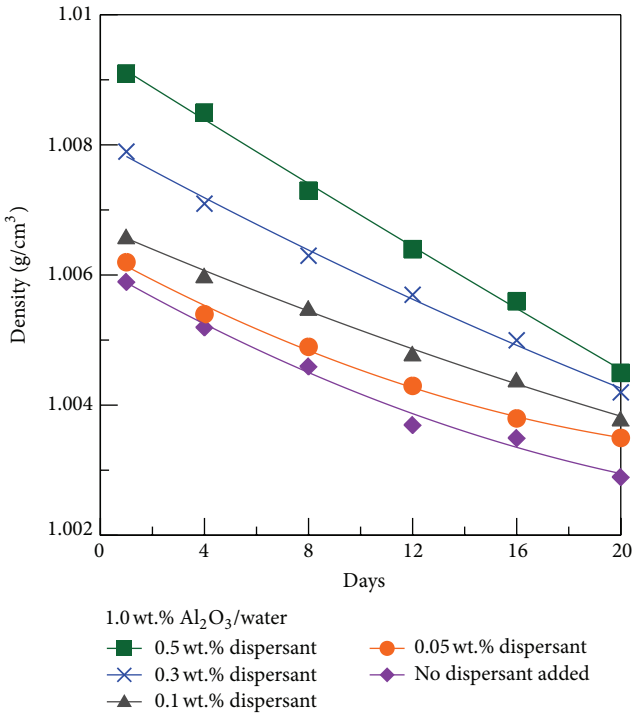

FIGURE 4: Correlation between weight concentration and precipitation behavior (1.0 wt.% Al_2O_3/water).

Table 2: Analysis of the component of copper surface in operation.

Concentration of nanofluid	Dispersant added	Surface distribution	Component analysis
0.5 wt.% Al_2O_3/water	No dispersant added		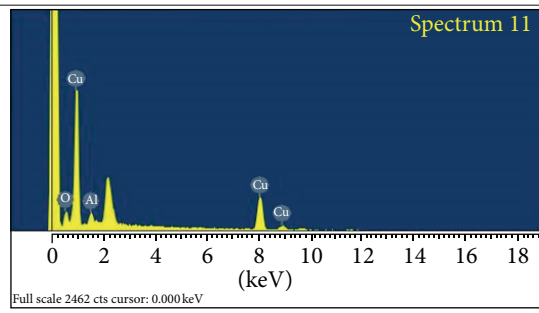
	0.05 wt.% cationic chitosan dispersant added		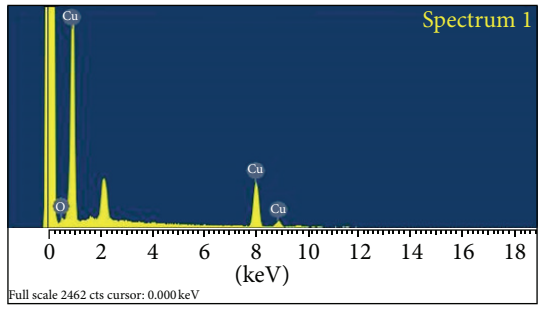
1.0 wt.% Al_2O_3/water	No dispersant added		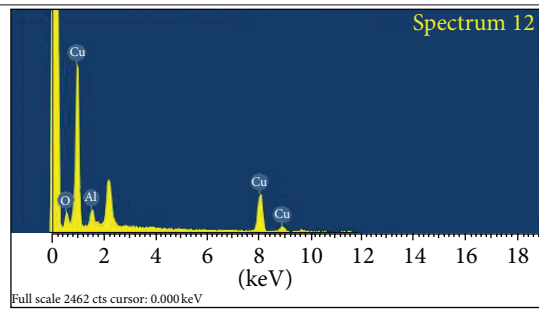
	0.05 wt.% cationic chitosan dispersant added		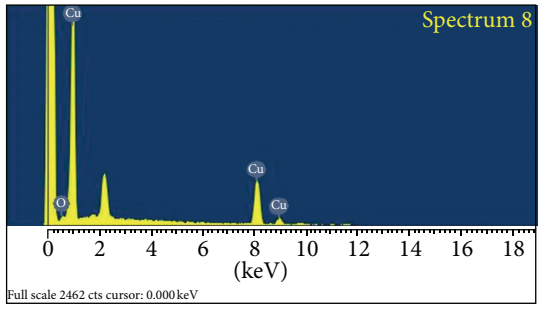

trend of particle adhesion on the surface. The surface of copper pipe had no significant powder particle adhesion after operating the nanofluid with dispersant. The study employed energy dispersive spectrometer to analyze the surface of copper, showing that nondispersant fluid sample resulted in the aluminum adhering to the surface of copper, but fluid with cationic chitosan dispersant prevented the aluminum from adhering to the surface of copper. The results suggested that nanofluid with cationic chitosan dispersant effectively reduced the possibility of nanoparticles adhering to the surface of copper and copper wall. This result also estimated that nanofluid with cationic chitosan dispersant reduced agglomeration in the pipeline in practical system operation.

Figures 6, 7, 8, and 9, respectively, indicate the increasing trend of the overall heat transfer capacity ratio of nanofluid at different flow rates and heating power. The results suggested that the increasing trend of the overall heat transfer capacity ratio resembled the heat conductivity ratio. Deionized nanofluid without dispersant showed higher increasing trend than deionized nanofluid with cationic chitosan dispersant under all operating conditions, but difference in trends of the overall heat transfer capacity ratio was less significant in the same power concentration than in trends of thermal conductivity ratio analysis. The dispersant improved the agglomeration and suspension of nanofluid, so the contact area and convection of heat exchange were promoted. The

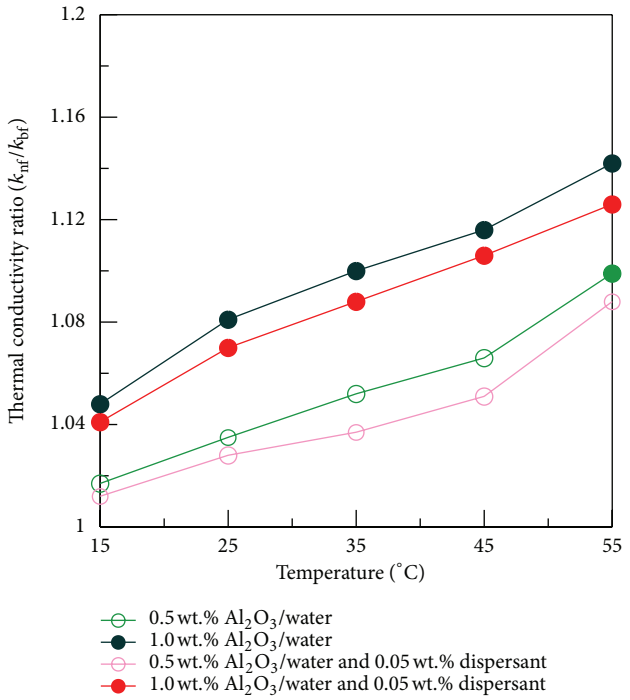

Figure 5: Correlations between temperature and thermal conductivity.

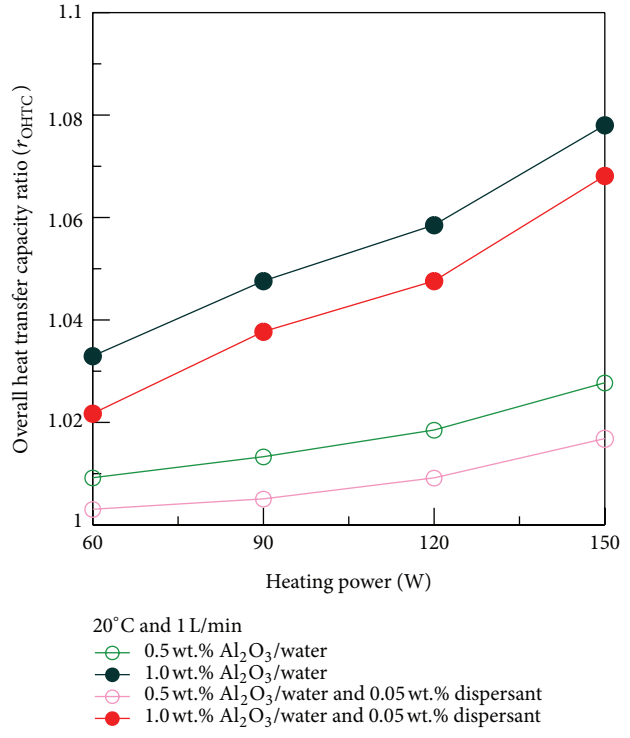

Figure 6: Increment of overall heat transfer capacity (20°C and 1 L/min).

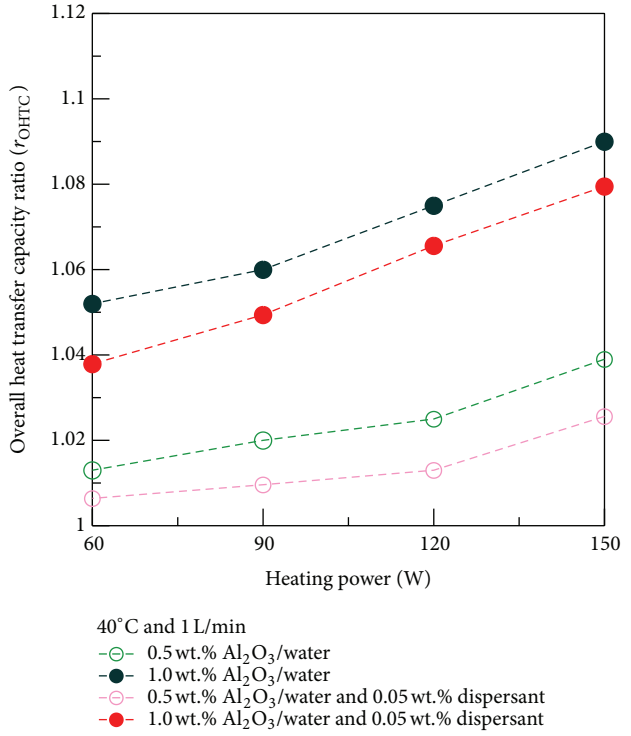

Figure 7: Increment of overall heat transfer capacity (40°C and 1 L/min).

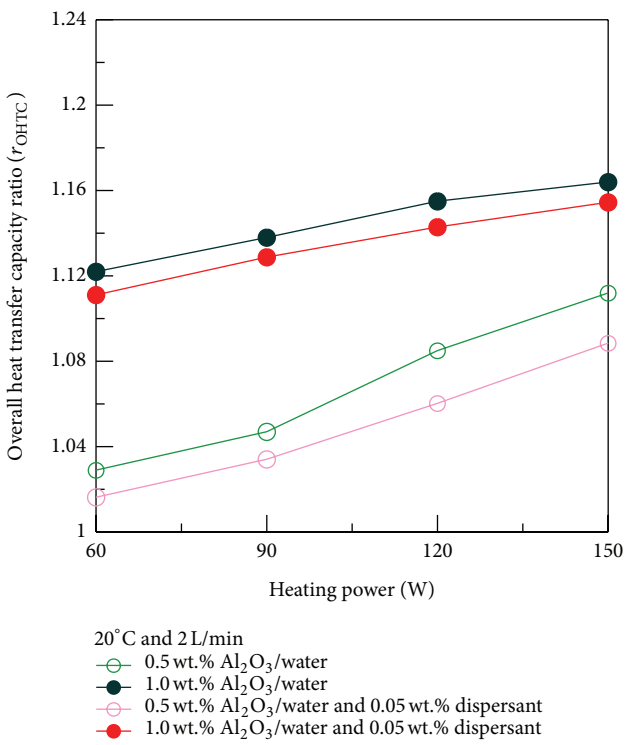

Figure 8: Increment of overall heat transfer capacity (20°C and 2 L/min).

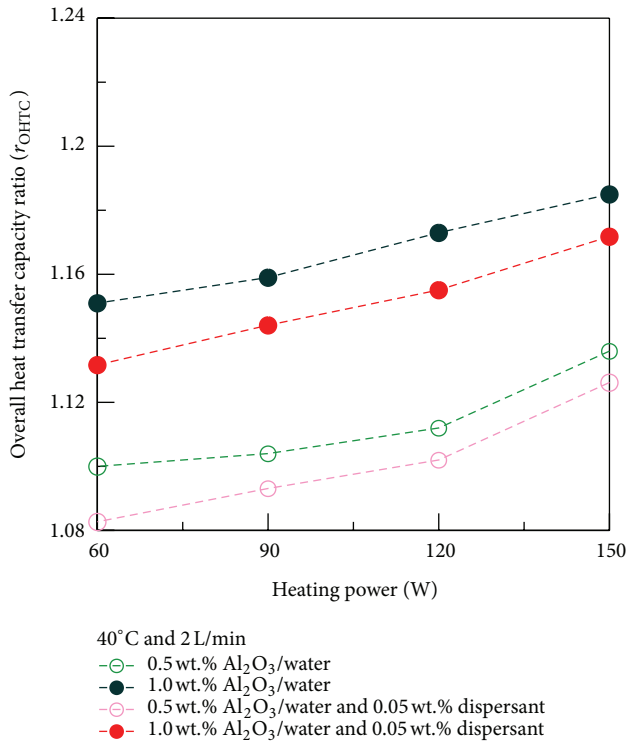

FIGURE 9: Increment of overall heat transfer capacity (40°C and 2 L/min).

overall heat transfer capacity ratio of 1.0 wt.% Al_2O_3/water nanofluid with 0.05 wt.% cationic chitosan dispersant was 17.4% at the flow ratio of 2 L/min heated by 150 W power and 8.3% heated by 60 W power.

5. Conclusions

Adding appropriate amount of cationic chitosan dispersant to the Al_2O_3/water nanofluid yielded the following results.

(1) It improved the agglomeration and precipitation of nanofluid by elevating the dispersion and suspension of nanofluid.

(2) It effectively reduced the risks of pipe blockage resulting from nanoparticles adhering to the pipe wall in the process of operation.

(3) Comparing with deionized water, the 1.0 wt.% Al_2O_3/water nanofluid had, respectively, 4.1% and 12.6% thermal conductivity at the temperature of 15°C and 55°C. At the flow ratio of 2 L/min, increment of overall heat transfer capacity, respectively, reached 8.3% and 17.4% when the nanofluid was heated by 60 W power and 150 W power.

Acknowledgment

This project is financially sponsored by the National Science Council under Grant NSC-98-2221-E-027-088-MY3.

References

[1] Y. H. Hung, T. P. Teng, and B. G. Lin, "Evaluation of the thermal performance of a heat pipe using alumina nanofluids," *Experimental Thermal and Fluid Science*, vol. 44, pp. 504–511, 2013.

[2] T. Yousefi, F. Veysi, E. Shojaeizadeh, and S. Zinadini, "An experimental investigation on the effect of Al_2O_3/H_2O nanofluid on the efficiency of flat-plate solar collectors," *Renewable Energy*, vol. 39, no. 1, pp. 293–298, 2012.

[3] D. P. Kulkarni, R. S. Vajjha, D. K. Das, and D. Oliva, "Application of aluminum oxide nanofluids in diesel electric generator as jacket water coolant," *Applied Thermal Engineering*, vol. 28, no. 14-15, pp. 1774–1781, 2008.

[4] C.-S. Jwo, L.-Y. Jeng, T.-P. Teng, and C.-C. Chen, "Performance of overall heat transfer in multi-channel heat exchanger by alumina nanofluid," *Journal of Alloys and Compounds*, vol. 504, pp. S385–S388, 2010.

[5] G. Huminic and A. Huminic, "Application of nanofluids in heat exchangers: a review," *Renewable and Sustainable Energy Reviews*, vol. 16, pp. 5625–5638, 2012.

[6] Y.-H. Hung, T.-P. Teng, T.-C. Teng, and J.-H. Chen, "Assessment of heat dissipation performance for nanofluid," *Applied Thermal Engineering*, vol. 32, no. 1, pp. 132–140, 2012.

[7] S. U. S. Choi and J. A. Eastman, "Enhancing thermal conductivity of fluids with nanoparticles," in *Proceedings of the International Mechanical Engineering Congress and Exhibition*, San Francisco, Calif, USA, 1995.

[8] J. A. Eastman, U. S. Choi, S. Li, L. J. Thompson, and S. Lee, "Enhanced thermal conductivity through the development of nanofluids," *Materials Research Society Symposium*, vol. 457, pp. 9–10, 1997.

[9] S. Lee, S. U.-S. Choi, S. Li, and J. A. Eastman, "Measuring thermal conductivity of fluids containing oxide nanoparticles," *Journal of Heat Transfer*, vol. 121, no. 2, pp. 280–288, 1999.

[10] X. Wang, X. Xu, and S. U. S. Choi, "Thermal conductivity of nanoparticle—fluid mixture," *Journal of Thermophysics and Heat Transfer*, vol. 13, no. 4, pp. 474–480, 1999.

[11] Y. Xuan and Q. Li, "Heat transfer enhancement of nanofluids," *International Journal of Heat and Fluid Flow*, vol. 21, no. 1, pp. 58–64, 2000.

[12] J. A. Eastman, S. U. S. Choi, S. Li, W. Yu, and L. J. Thompson, "Anomalously increased effective thermal conductivities of ethylene glycol-based nanofluids containing copper nanoparticles," *Applied Physics Letters*, vol. 78, no. 6, pp. 718–720, 2001.

[13] C. H. Li and G. P. Peterson, "Experimental investigation of temperature and volume fraction variations on the effective thermal conductivity of nanoparticle suspensions (nanofluids)," *Journal of Applied Physics*, vol. 99, no. 8, Article ID 084314, 2006.

[14] D.-H. Yoo, K. S. Hong, and H.-S. Yang, "Study of thermal conductivity of nanofluids for the application of heat transfer fluids," *Thermochimica Acta*, vol. 455, no. 1-2, pp. 66–69, 2007.

[15] C. H. Li and G. P. Peterson, "The effect of particle size on the effective thermal conductivity of Al_2O_3-water nanofluids," *Journal of Applied Physics*, vol. 101, no. 4, Article ID 044312, 2007.

[16] K.-F. V. Wong and T. Kurma, "Transport properties of alumina nanofluids," *Nanotechnology*, vol. 19, no. 34, Article ID 345702, 2008.

[17] S. E. B. Maiga, C. T. Nguyen, N. Galanis, and G. Roy, "Heat transfer behaviours of nanofluids in a uniformly heated tube," *Superlattices and Microstructures*, vol. 35, no. 3–6, pp. 543–557, 2004.

[18] S. E. B. Maiga, S. J. Palm, C. T. Nguyen, G. Roy, and N. Galanis, "Heat transfer enhancement by using nanofluids in forced convection flows," *International Journal of Heat and Fluid Flow*, vol. 26, no. 4, pp. 530–546, 2005.

[19] S. K. Das, N. Putra, P. Thiesen, and W. Roetzel, "Temperature dependence of thermal conductivity enhancement for nanofluids," *Journal of Heat Transfer*, vol. 125, no. 4, pp. 567–574, 2003.

[20] C. H. Chon and K. D. Kihm, "Empirical correlation finding the role of temperature and particle size for nanofluid (Al_2O_3) thermal conductivity enhancement," *Applied Physics Letters*, vol. 87, no. 15, Article ID 153107, pp. 1–3, 2005.

[21] C. Kang, M. Okada, A. Hattori, and K. Oyama, "Natural convection of water-fine particle suspension in a rectangular vessel heated and cooled from opposing vertical walls (classification of the natural convection in the case of suspension with a narrow-size distribution)," *International Journal of Heat and Mass Transfer*, vol. 44, no. 15, pp. 2973–2982, 2001.

[22] X.-J. Wang, O.-S. Zhu, and S. Yang, "Investigation of pH and SDBS on enhancement of thermal conductivity in nanofluids," *Chemical Physics Letters*, vol. 470, no. 1–3, pp. 107–111, 2009.

[23] W. Yu and H. Xie, "A review on nanofluids: preparation, stability mechanisms, and applications," *Journal of Nanomaterials*, vol. 2012, Article ID 435873, 17 pages, 2012.

[24] D. S. Zhu, X. F. Li, N. Wang, X. J. Wang, J. W. Gao, and H. Li, "Dispersion behavior and thermal conductivity characteristics of Al_2O_3-H_2O nanofluids," *Current Applied Physics*, vol. 9, no. 1, pp. 131–139, 2009.

[25] K. Wusiman, H. Jeong, K. Tulugan, H. Afrianto, and H. Chung, "Thermal performance of multi-walled carbon nanotubes (MWCNTs) in aqueous suspensions with surfactants SDBS and SDS," *International Communications in Heat and Mass Transfer*, vol. 41, pp. 28–33, 2013.

[26] R. Mondragon, J. E. Julia, A. Barba, and J. C. Jarque, "Characterization of silica-water nanofluids dispersed with an ultrasound probe: a study of their physical properties and stability," *Powder Technology*, vol. 224, pp. 138–146, 2012.

[27] D. D. Ebbing and S. D. Gammon, *General Chemistry*, Cengage, 2013.

[28] S. K. Das, S. U. S. Choi, W. Yu, and T. Pradeep, *Nanofluids Science and Technology*, John Wiley & Sons, 2008.